

Electrochemical and Spectroscopic Properties of Cyclometallated and Non-Cyclometallated Ruthenium(II) Complexes Containing Sterically Hindering Ligands of the Phenanthroline and Terpyridine Families

Francesco Barigelletti,^{*[a]} Barbara Ventura,^[a] Jean-Paul Collin,^{*[a]} Robert Kayhanian,^[a] Pablo Gaviña,^{[a][†]} and Jean-Pierre Sauvage^[a]

Keywords: Ruthenium / Phenanthroline / Luminescence / Sterically hindered ligands / Terpyridine / Cyclometallation

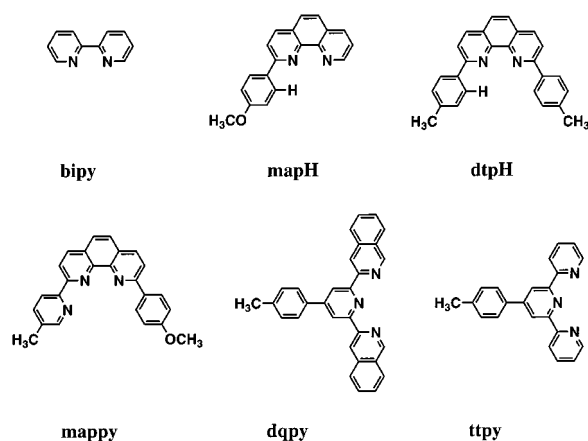
Two series of cyclometallated and noncyclometallated ruthenium(II) complexes incorporating mono- or disubstituted 1,10-phenanthroline- and 2,2':6',2''-terpyridine-type ligands have been synthesized and characterized. An X-ray crystal structure for one of the complexes, Ru(tpy)(mapH)(Cl)(PF₆), has been obtained (mapH = 2-*p*-anisyl-1,10-phenanthroline; tpy = 4'-tolyl-2,2':6',2''-terpyridine). Distinct electrochemical and photophysical properties have been

observed for the two series: a remarkable feature is the observation of relatively long-lived MLCT excited states (from 70 to 106 ns at room temperature in CH₃CN) for three of the cyclometallated complexes. A discussion is given on the role of factors like sigma donation by the cyclometallating ligands, interligand steric hindrance and interligand π - π interactions that affect the electrochemical and spectroscopic properties.

Introduction

The photophysical behavior of transition metal polypyridine complexes is of prime importance in molecular devices based on photoinduced electron and energy transfer reactions.^[1] Numerous studies on complexes exhibiting luminescence from metal-to-ligand charge-transfer (MLCT) excited states have shown the determining effects of different factors on the excited state properties.^[2] Among others, the energy level of the low-lying states (energy gap law),^[3] the electron delocalization on the acceptor ligand,^[4] as related to its structure and rigidity^[5] have been correlated with parameters like absorption and luminescence wavelengths, lifetime and quantum yield. With the aim of developing new approaches to the tuning of excited-states properties, we have prepared a series of ruthenium(II) complexes incorporating cyclometallated and noncyclometallated sterically hindering ligands. In these complexes, the electron density distribution associated with the presence of cyclometallating positions may result in improved luminescence properties, as illustrated below for some of the compounds investigated. We also show that the interligand interactions between hindering ligands can play a non-negligible role in determining the luminescence properties^[6] provided that the steric constraint does not distort excessively the octahedral coordination. The schematic structures of the relevant ligands are illustrated in Scheme 1. A preliminary re-

port of some properties of compounds **4**, **7**, and **9** has been published previously.^[7]



Scheme 1

Results and Discussion

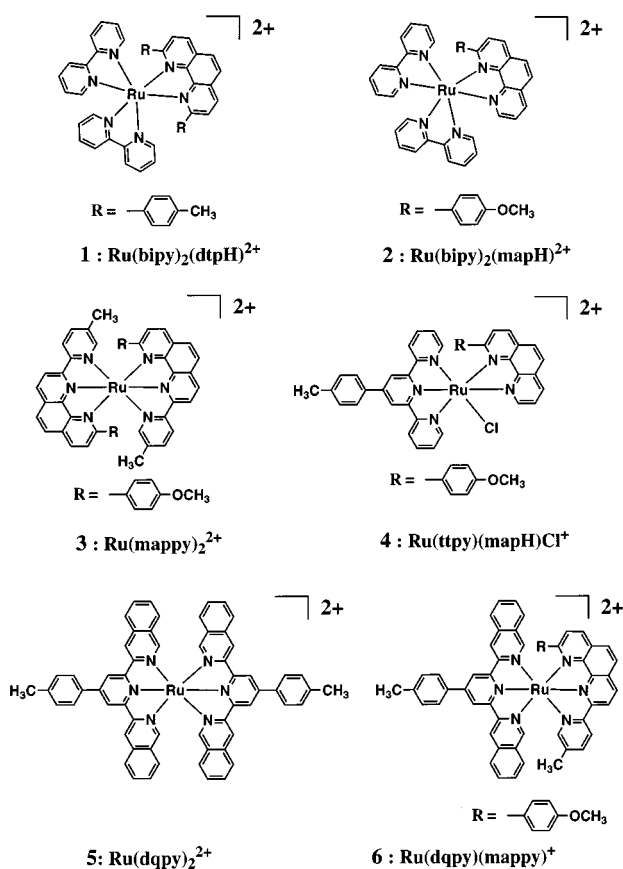
The ruthenium complexes synthesized and studied are represented in Scheme 2 (**1–6**: noncyclometallated compounds) and Scheme 3 (**7–10**: cyclometallated compounds). Cyclometallated ruthenium(II) complexes involving ligands that contain a phenyl group adjacent to a nitrogen donor atom are relatively easy to obtain.^[8] Depending on the potential donor atoms implied and the experimental conditions, the complexation reaction leads to the normal N₆ coordination sphere or to the N₅C set.^[9] The reaction of paramagnetic ruthenium(III) species (RuLCl₃; L = tpy, dqpy or mappy) with one equivalent of hindering phenanthroline (mapH, dtpH or mappy) in refluxing glacial acetic acid in the presence of a mild reducing agent (*N*-ethylmorpholine) gave the complexes **3** to **10**. In the case of

^[a] Istituto FRAE-CNR, via P. Gobetti 101, I-40129 Bologna, Italy

^[b] Laboratoire de Chimie Organo-minérale, Institut Le Bel, Université Louis Pasteur, 4 rue Blaise Pascal, F-67070 Strasbourg, France
E-mail: sauvage@chimie.u-strasb.fr

^[†] Present address: Departament de Química Orgànica, Universitat de València, Facultat de Farmàcia, Av. Vicent Andrés Estellés s/n, E-16100 Burjassot (València), Spain

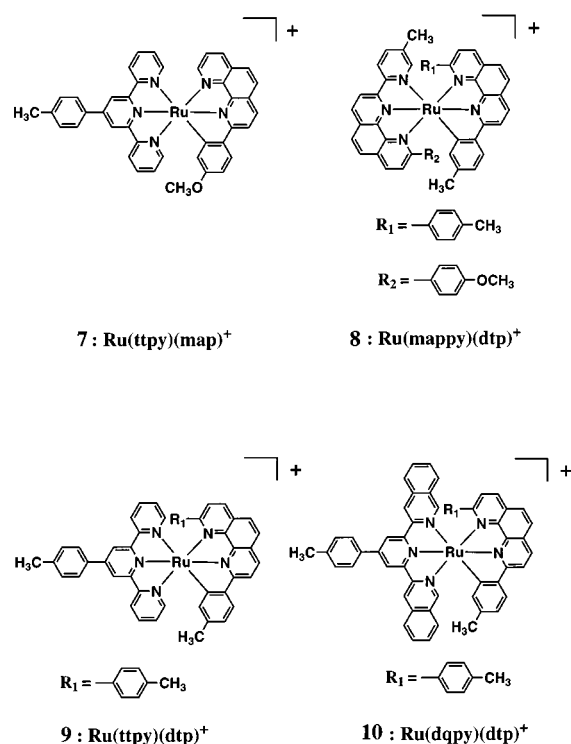
complexes **1** and **2**, the ruthenium precursor was Ru(bipy)₂Cl₂. All the compounds were characterized by ¹H-NMR and FAB-MS spectra and these data are in full agreement with their postulated structures.



Scheme 2

The X-ray structures of **7** and **9** have already been reported.^[7] Single crystals of **4** were obtained by crystallization from a mixture acetonitrile and benzene. The ORTEP diagram of **4** is shown in Figure 1. Selected bond lengths and bonds angles are presented in Table 1. For comparison purposes some data concerning **7** and **9** are also given.

The ruthenium ligand environment exhibits a distorted octahedral geometry with the terpyridine ligand coordinated in meridional configuration. The phenanthroline plane is orthogonal to the terpyridine mean plane whereas the anisyl substituent is in a stacking position with the central pyridine of the terpyridine (the angle between these rings is 4.2° and the distance between planes is around 3.4 Å). The chloride ion is directed from the N2 nitrogen atom of the phenanthroline. The Ru–Cl bond length of 2.391 Å is very similar to that reported for other ruthenium terpyridine chloro complexes, such as 2.405 Å for Ru(terpy)(bpz)Cl⁺^[10] (bpz = 2,2'-bipyrazine) and 2.400 Å for [Ru(terpy)(CO)₂Cl]Cl.^[11] The terpyridine ligand affords two almost identical Ru–N bond lengths of ca. 2.05 Å (Ru–N3 and Ru–N5) whereas the distance Ru–N4 is shorter for the central pyridine (1.950 Å). The two side pyridines bind to ruthenium at angles of 79.3° (N3–Ru–N4)



Scheme 3

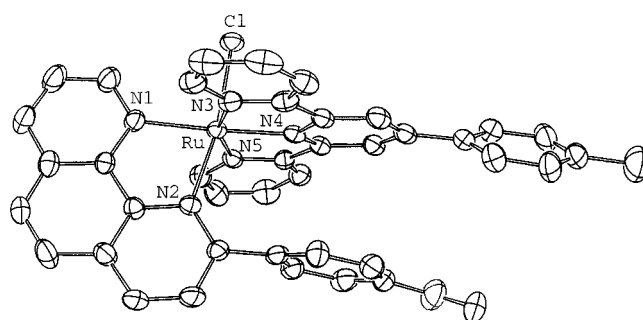


Figure 1. ORTEP representation of the X-ray structure of **4**. The hydrogen atoms and PF₆ anion have been omitted for clarity. Thermal ellipsoids are scaled to enclose 30% of the electronic density

and 79.8° (N4–Ru–N5) and these angles also show that terpyridine is constrained such that it cannot fit with an ideal (90°) geometry.

Contrary to what was observed in compound **7** and **9**^[7] the Ru–N1 and Ru–N2 bond lengths are in agreement with the usual coordination of the substituted phenanthroline to the ruthenium. In fact, for **7** and **9**, the unusually long Ru–N1 (for **7**) and Ru–N2 (for **9**) bond lengths (2.198 Å and 2.256 Å, respectively) could be the consequence of a *trans* effect (due to the carbon atom in the *trans* position) as well as the constrained geometry inherent in terpyridine-type chelate.

The electrochemical data for the noncyclometallated (**1** to **6**) and cyclometallated (**7** to **10**) ruthenium complexes are presented in Table 2. Oxidations are metal-centered and reductions are ligand-centered processes respectively. Reversible monoelectronic waves are observed for almost all

Table 1. Selected bond lengths and bond angles for **4**, **7** and **9** (numbers in parentheses are estimated standard deviations in the least significant digits)

	Bonds lengths [Å]		Bonds angles [°]	
4	Ru–Cl	2.3917(8)	Cl–Ru–N1	91.89(8)
	Ru–N1	2.078(3)	N1–Ru–N2	79.2(1)
	Ru–N2	2.087(3)	N1–Ru–N3	100.8(1)
	Ru–N3	2.067(3)	N1–Ru–N4	176.6(1)
	Ru–N4	1.953(2)	N3–Ru–N4	79.3(1)
7	Ru–N5	2.043(3)	N4–Ru–N5	79.8(1)
	Ru–N1	2.198(6)	N1–Ru–N2	76.9(2)
	Ru–N2	2.009(6)	N1–Ru–C18	156.0(3)
	Ru–C18	2.030(8)	N1–Ru–N3	93.7(2)
	Ru–N3	2.050(5)	N1–Ru–N4	105.4(2)
9	Ru–N4	1.961(6)	N1–Ru–N5	91.5(2)
	Ru–N5	2.062(5)	N2–Ru–C18	79.1(3)
	Ru–N1	2.010(2)	N1–Ru–N2	76.6(1)
	Ru–N2	2.256(3)	N1–Ru–C18	78.3(1)
	Ru–N3	2.031(3)	N1–Ru–N3	100.6(1)
	Ru–N4	1.942(3)	N3–Ru–N4	79.8(1)
	Ru–N5	2.052(2)	N4–Ru–C18	93.5(1)
	Ru–C18	2.037(4)	N2–Ru–N4	111.5(1)

redox couples. As expected, compounds **1**, **2** and **3** display redox processes typical of the well-known bipyridine, phenanthroline, and terpyridine complexes.^[1] In compound **4**, due to the coordinated chloride ion, the ruthenium is easier to oxidize (by 500 mV as compared to **3**) and one ligand is more difficult to reduce. In compounds **5** and **6**, the presence of electron-withdrawing quinoline ligands provides a slightly higher acceptor character to these complexes than the classical bis(terpyridine) compound.

Table 2. Redox potentials (vs SCE) measured by cyclic voltammetry. Conditions: CH₃CN (*n*Bu₄NBF₄ = 0.1 M), ν = 100 mV s⁻¹, room temperature.

	Ru ^{III/II}	L ^{0/-}	L ⁻²⁻	L ^{2-/-3-}
1	1.27	-1.33	-1.60	
2	1.27	-1.33	-1.52	
3	1.29	-1.16	-1.42	-1.91
4	0.77	-1.50	-1.85 ^[b]	
5	1.14	-1.36	-1.52	
6	1.08	-1.19	-1.56	-1.82
7	0.54	-1.54	[a]	
8	0.57	-1.47	[a]	
9	0.54	-1.57	[a]	
10	0.44	-1.63	-1.83	2.08 ^[b]

[a] Large cathodic current occurs without distinctive peak. – [b] Irreversible.

For complexes **7** to **10**, the effect of the cyclometallation on the stability of the Ru^{III} state is illustrated by a cathodic shift of 750 mV. This behavior demonstrates the strong σ -donating character of the anionic (map⁻ or dtp⁻) ligands. The ligand-centered reduction is also strongly affected by the presence of the cyclometallating ligand. In fact, the first reduction in these compounds occurs at around -1.6 V while it occurs around -1.3 V for **1** and **2**.

The absorption maxima, the molar absorption coefficients and the luminescence properties in acetonitrile and

in butyronitrile are collected in Table 3 and representative absorption spectra in the series are shown in Figure 2.

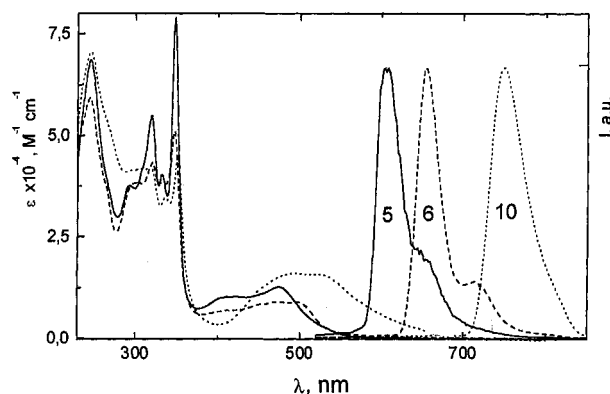


Figure 2. Absorption spectra (acetonitrile, room temperature) and normalized luminescence spectra (butyronitrile, 77 K) of complexes **5**, **6**, and **10**

The absorption bands in the UV region are ascribed to ligand-centered transitions (¹LC) and those occurring in the visible part, with ϵ around 10⁴ M⁻¹ cm⁻¹, correspond to ¹MLCT transitions.^[1a] In the case of the cyclometallated complexes (**7**–**10**) the absorption bands occurring at low energy (495 to 527 nm) could be attributed to MLCT transitions involving the LUMO of the noncyclometallating ligand, i.e. ttpy (case of **7**, **9**, **10**) or mappy (case of **8**). Actually, as has already been established,^[12] the level of the LUMO for the cyclometallated (anionic) ligand is expected to be higher in energy than that of an isoelectronic but neutral polypyridine ligand.

All the ruthenium complexes exhibit an intense luminescence at 77 K in butyronitrile (Table 3). The luminescence band maxima for the cyclometallated complexes are bathochromically shifted with respect to the noncyclometallated compounds. At room temperature, in CH₃CN, a more distinct behavior appears between the two series. Whereas compounds **1** and **3**–**6** are nonluminescent, as found for many tpy-containing derivatives,^[1c] the cyclometallated complexes **8**, **9** and **10** luminesce and display relatively long-lived excited states (from 70 to 106 ns). This behavior can be understood in terms of the interplay of MLCT and metal-centered (MC) excited states, as discussed below.

In the case of ruthenium terpyridine-type complexes the distorted octahedral geometry induces a relatively weak ligand field at the metal center.^[1c] As a consequence, effective pathways for deactivation of the ³MLCT state are established by population of thermally accessible upper-lying ³MC states. This effect is likely to be enhanced by the presence of bulky substituents in the α -position with respect to the N atom (case of **3** and **6**). This type of argument also could be used to explain the behavior of **1**, in which 2,9-bis-*p*-tolyl-1,10-phenanthroline is associated with a Ru-(bipy)₂ core. In contrast, if the coordination sphere of the metal is less constrained as in **2**, a sizable luminescence can be observed.

Table 3. Spectroscopic properties^[a]

Absorption λ_{\max} [nm] (ϵ [$M^{-1} \text{ cm}^{-1}$])				Luminescence				
			λ_{\max} [nm]	293 K τ [ns]	293 K Φ	293 K λ_{\max} [nm]	77 K τ [μ s]	77 K
1		452 (10200)	288 (46000)	—	—	—	602	6.6
2		448 (10500)	288 (44000)	618	3.4	5.6×10^{-3}	586	6.2
3	503 (9100)	344 (36000)	300 (41200)	—	—	—	646	9.3
4		508 (13400)	285 (48500)	—	—	—	790	0.8
5		473(12700)	348 (79000)	—	—	—	605	17.2
6	495 (8900)	474 (9000)	347 (51000)	—	—	—	655	11.3
7	518 (17800)	355 (26500)	309 (39000)	—	—	—	704	3.6
8	523 (8600)	440 (6700)	314 (35000)	816	106	1.9×10^{-3}	814	2.3
9	527 (16300)	388 (12000)	316 (43000)	802	95	2.0×10^{-2}	778	2.6
10	520 (15700)	493 (16000)	351 (44000)	778	70.5	2.8×10^{-4}	750	3.4

^[a] Acetonitrile solvent at room temperature, butyronitrile at 77 K.

In the case of cyclometallated ruthenium complexes it has already been recognized^[13] that the strong ligand field provided by σ -donation at the carbon coordination increases the energy gap between the lowest-lying ³MLCT levels (which involve the noncyclometallating ligand) and the upper-lying ³MC states. This increase is basically due to a loading of electron density at the metal center, which results both in destabilization of the ³MC level and stabilization of the ³MLCT level (as indicated by the values of the luminescence band maxima at 77 K, Table 3). It is noteworthy that, according to the "energy-gap law", the latter effect is expected to enhance the nonradiative processes from the emitting state.^[3] In the case of **8**, **9** and **10**, the balance of these effects results in sizable luminescence at room temperature, which is not the case for most of the terpyridine-containing ruthenium complexes.^[1c] We noticed that, for **8**, **9**, and **10**, large ligand fragments undergoing interligand π - π interactions are present,^[7] which can assist an extended electron delocalization for the MLCT states and result in the known beneficial effects noted in the case of large rigid ligands.^[4] By contrast, the Ru(ttpy)(map)⁺ (**7**) complex, which is necessarily devoid of such interligand interactions, does not luminesce at room temperature (Table 3).

Experimental Section

Physical Measurements: ¹H NMR: Bruker WP200 SY (200 MHz). – UV/Vis: Kontron Uvikon 860. – MS: VG ZAB-HF, Thomson THN 208. – Cyclic voltammetry data: PAR model 273A potentiostat, Pt disk as working electrode, CH₃CN solution, 0.1 M Bu₄NBF₄ as supporting electrolyte, Pt wire as auxiliary electrode, SCE as reference electrode.

Photophysical Measurements: Absorption spectra were determined with a Perkin–Elmer Lambda 5 spectrometer. – Uncorrected luminescence spectra were obtained from a Spex Fluorolog II fluorimeter equipped with a Hamamatsu R928 phototube. Uncorrected band maxima are used throughout the text. The luminescence quantum yields, Φ , were obtained from dilute solutions (the absorbance at the selected excitation wavelength was < 0.1)^[20a] by analysing spectra that were corrected for the photomultiplier response and by comparison with the spectrum of Ru(bpy)₃²⁺ (Φ = 0.028 in aerated water).^[20b] Luminescence lifetimes were obtained

with an IBH single photon apparatus employing a lamp filled with N₂; the decays were found to follow a single exponential behavior in each case. Further details were given elsewhere.^[21] The experimental uncertainties were estimated to be 2 nm for the absorption and luminescence spectra, 20% for the luminescence intensities and 10% for the luminescence lifetimes.

Materials and General Procedures: The following chemicals were prepared according to literature procedures: 2-*p*-anisyl-1,10-phenanthroline (**mapH**);^[14] 2,9-bis(*p*-tolyl)-1,10-phenanthroline (**dtpH**);^[15] 4'-tolyl-2,2',6',2''-terpyridine (**ttpy**);^[16] Ru(bp)₂Cl₂·2H₂O;^[17] Ru(ttpy)Cl₃.^[18]

2-*p*-Anisyl-9-(4-methyl-2-pyridyl)-1,10-phenanthroline (mappy**):** To a degassed solution of 2-bromo-5-methylpyridine (0.757 g, 4.4 mmol) in dry ether (15 mL) at –78 °C was added dropwise *n*BuLi (soln. in hexane approx. 1.3 M, 3.7 mL, 4.84 mmol). The resulting red solution was warmed to –40 °C and stirred at this temperature, under Ar, for 30 min. The organolithic solution was then transferred, by cannula, to a degassed solution of 2-*p*-anisyl-1,10-phenanthroline (1.145 g, 4.0 mmol) in dry ether (35 mL) at 0 °C. The mixture was stirred under argon for 3 h at 0 °C and then for a further 3 h at 10 °C. After hydrolysis at 0 °C with water (15 mL), the organic layer was decanted and the aqueous layer extracted with dichloromethane. The combined organic layers were rearomatized by successive additions of MnO₂ (3 × 3 g, 3 g each 20 min), dried over MgSO₄ and filtered. After evaporation of the solvent the crude product was purified by column chromatography on alumina, with dichloromethane as eluent. The product, **mappy**, was obtained as a pale yellow solid (0.89 g, 59%). The solid crystallized from ethanol to give pale yellow crystals (m.p. 243.5–245.0 °C). – ¹H NMR (200 MHz, CDCl₃): δ = 9.00 (d, J = 8.2 Hz, 1 H, H³), 8.82 (d, J = 8.4 Hz, 1 H, H³), 8.58 (d, J = 2.2 Hz, 1 H, H⁶), 8.45 (d, J = 8.9 Hz, 2 H, 2 H^o), 8.36 (d, J = 8.4 Hz, 1 H, H⁴), 8.29 (d, J = 8.5 Hz, 1 H, H⁷), 8.11 (d, J = 8.5 Hz, 1 H, H⁸), 7.81 (dd, J = 8.2 and 2.2 Hz, 1 H, H⁴), 7.79 (s, 2 H, H^{5,6}), 7.13 (d, J = 8.9 Hz, 2 H, 2 H^m), 3.94 (s, 3 H), 2.46 (s, 3 H). – Anal. calcd. for C₂₅H₁₉N₃O (377.45): C 79.55, H 5.07, N 11.13; found: C 79.30, H 5.26, N 11.17.

3-Acetylisquinoline: To sodium ethoxide (0.27 g, 0.012 mol) in dry benzene (40 mL) was added, with stirring, a mixture of methyl 3-isoquinoline carboxylate (1.8 g, 9.6 mmol) and anhydrous ethyl acetate (1.14 g, 15.8 mmol) in benzene (35 mL). The mixture was allowed to reflux with stirring for 24 h. The mixture was allowed to cool to room temperature and poured into a solution of sodium hydroxide (0.40 g, 0.01 mol) in water (7 mL). The light yellow solid that separated on the addition of the base was filtered off and water

(20 mL) was added to the filtrate. After decantation of the phases, the benzene layer was washed with water and the combined aqueous layer was extracted with ether (3 × 30 mL). The combined organic layers were evaporated and combined with the light yellow solid. To this was added concentrated hydrochloric acid and the mixture was heated to reflux for 2 h. On cooling, the mixture was made basic with sodium carbonate, the organic layer was extracted with ether (2 × 40 mL) and dried over sodium sulfate. Removal of the ether and purification on silica (dichloromethane/hexane 80:20) gave 1.23 g (75%) of 3-acetyl-isoquinoline. – ¹H NMR (200 MHz, CDCl₃): δ = 9.26 (s, 1 H), 8.45 (s, 1 H), 8.05–7.94 (m, 2 H), 7.79–7.67 (m, 2 H), 2.80 (s, 3 H). – MS (EI); *m/z*: 171.

2,6-Diisoquinoyl-(4-tolyl)pyridine (dqpy): To a dried sample of 3-acetyl-isoquinoline (1.23 g, 7.19 mmol), ammonium acetate (3.6 g, 46.7 mmol) and acetamide (5.54 g, 93.8 mmol) was added *p*-tolualdehyde (0.37 g, 3.11 mmol). The mixture was heated with stirring to 170 °C under solvent-free conditions under an atmosphere of argon for 3 h. After this time the temperature of the reaction mixture was lowered to 120 °C and the mixture was added to a solution of sodium hydroxide (2.8 g, 0.07 mol) in water (10 mL), a process that resulted in a brownish oil. The mixture was left at this temperature for a further 2 h. The dark brown oil and the yellow hot solution was poured into a beaker and, after cooling, the brown oil solidified. The solid was dissolved in acetic acid (10 mL) and refluxed for 2 h. 47% hydrobromic acid (10 mL) was then added and the mixture was left to stir at room temperature for a further 2 h. After this time, addition of a 5 N solution of potassium hydroxide (20 mL) resulted in the formation of a precipitate. The organic layer was extracted with dichloromethane (3 × 60 mL) and the combined organic layers were washed with sodium hydrogen carbonate and dried over magnesium sulfate. After column chromatography on alumina (hexane/ether; 8:2), dqpy was obtained as a white material (1.3 g, 43%). – ¹H NMR (300 MHz, CDCl₃): δ = 9.36 (s, 2 H), 9.08 (s, 2 H), 8.83 (s, 2 H), 8.08 (d, 2 H, *J* = 7.29 Hz), 8.03 (d, 2 H, *J* = 8.04 Hz), 7.87 (d, 2 H, *J* = 8.22 Hz), 7.74 (td, 2 H, *J* = 1.28 Hz), 7.63 (td, 2 H, *J* = 1.10 Hz), 7.33 (d, 2 H, *J* = 7.86 Hz), 2.43 (s, 3 H). – MS (EI); *m/z*: 423.2.

Ru(mappy)Cl₃: To absolute ethanol (30 mL) in a 100 mL round-bottomed flask was added RuCl₃·3H₂O (0.042 g, 0.132 mmol) and mappy (0.050 g, 0.132 mmol). The mixture was heated at reflux for 3 h with vigorous stirring. After this time, the reaction mixture was cooled to room temperature and the fine brown powder was collected by vacuum filtration, washed with cold absolute ethanol (3 × 30 mL) followed by Et₂O (3 × 30 mL) and dried under vacuum to give 0.065 g (84%) of Ru(mappy)Cl₃.

Ru(dqpy)Cl₃: This compound was prepared in the same manner as for the analogous compound, Ru(mappy)Cl₃, in almost quantitative yield. The insoluble brown-red product obtained was used without further purification.

General Workup Procedure for the Complexes 1 to 10: After reaction, the solvent was removed under reduced pressure and the colored solid was redissolved in methanol. The colored solution was filtered to remove any trace of unchanged starting complex and the filtrate obtained was added to an aqueous solution of KPF₆ (0.5 g in 50 mL of water) to give a solid. This solid was purified by silica gel chromatography, eluting with a mixture of CH₂Cl₂/CH₃OH (95:5) for all the complexes excepted for **5**, where the elution was performed with a CH₃CN/H₂O/saturated KNO₃ mixture (100:10:1).

Ru(bipy)₂(dtpH)(PF₆)₂ (1): A suspension of Ru(bipy)₂Cl₂·2H₂O^[17] (0.065 g, 0.13 mmol) and dtpH (0.046 g, 0.13 mmol) in acetic acid (10 mL) with 2–3 drops of *N*-ethylmorpholine was refluxed under

argon for 3 h. Yield 0.033 g (24%). – ¹H NMR (200 MHz, CD₂Cl₂): δ = 8.56 (d, 2 H, *J* = 8.22 Hz), 8.28 (s, 2 H), 8.25 (d, 2 H, *J* = 8.22 Hz), 8.09 (td, 2 H, *J* = 6.21 Hz, *J* = 1.47 Hz), 7.82 (d, 2 H, *J* = 8.21 Hz), 7.78 (d, 2 H, *J* = 5.49 Hz), 7.70 (d, 2 H, *J* = 8.24 Hz), 7.52–7.39 (m, 4 H), 7.02 (br, 2 H), 6.65–6.61 (m, 7 H), 5.96 (br, 3 H), 2.16 (s, 6 H). – MS (FAB-MS) (nitrobenzyl alcohol matrix); *m/z* (%): 919 (20) [M – PF₆[–]], 774 (10) [M – 2PF₆[–] + e[–]], 617 (12) [M – 2PF₆[–] – bipy + e[–]].

Ru(bipy)₂(mapH)(PF₆)₂ (2): A suspension of Ru(bp)₂Cl₂·2H₂O (0.050 g, 0.096 mmol) and mapH (0.026 g, 0.09 mmol) in acetic acid (7 mL) with 2–3 drops of *N*-ethylmorpholine was refluxed under argon for 4 h. Yield 0.065 g (68%). – ¹H NMR (200 MHz, CD₂Cl₂): δ = 8.62 (d, 1 H, *J* = 8.4 Hz), 8.56 (dd, 1 H, *J* = 8.4 Hz, *J* = 1.29 Hz), 8.40 (d, 1 H, *J* = 7.86 Hz), 8.34 (d, 1 H, *J* = 7.50 Hz), 8.31–8.22 (m, 4 H), 8.07 (td, 1 H, *J* = 7.86 Hz, *J* = 8.01 Hz), 7.99–7.94 (m, 4 H), 7.91 (d, 1 H, *J* = 5.49 Hz), 7.74–7.62 (m, 4 H), 7.49–7.31 (m, 6 H), 7.29 (br, 1 H), 7.07 (d, 1 H, *J* = 5.67 Hz), 6.93 (t, 1 H, *J* = 7.11 Hz), 3.70 (s, 3 H). – MS (FAB-MS) (nitrobenzyl alcohol matrix); *m/z* (%): 845 (50) [M – PF₆[–]], 700 (35) [M – 2PF₆[–] + e[–]].

Ru(mappy)₂(PF₆)₂ (3): A suspension of Ru(mappy)Cl₃ (0.060 g, 0.10 mmol) and mappy (0.039 g, 0.10 mmol) was heated to reflux for 3 h in glacial acetic acid (6 mL) with 2–3 drops of *N*-ethylmorpholine. Yield 0.10 g (87%). – ¹H NMR (200 MHz, CD₂Cl₂): δ = 8.77 (d, 2 H, *J* = 8.6 Hz), 8.63 (d, 2 H, *J* = 8.6 Hz), 8.44 (t, 4 H, *J* = 8.06 Hz), 8.24 (s, 4 H), 7.69 (dd, 2 H, *J* = 8.20 Hz, *J* = 1.2 Hz), 7.36 (d, 2 H, *J* = 8.34 Hz), 6.23–6.19 (br, 2 H), 6.15 (s, 2 H), 5.93–5.63 (m, 6 H), 3.76 (s, 6 H), 1.89 (s, 6 H). – MS (FAB-MS) (nitrobenzyl alcohol matrix); *m/z* (%): 1001 (15) [M – PF₆[–]], 856 (24) [M – 2PF₆[–] + e[–]].

Ru(ttpy)(mapH)(Cl)(PF₆) (4) and Ru(ttpy)(map)(PF₆) (7): Ru(ttpy)Cl₃ (0.10 g, 0.19 mmol) and mapH (0.054 g, 0.19 mmol) were heated to reflux for 3 h in glacial acetic acid (6 mL) with 2–3 drops of *N*-ethylmorpholine. Yield: 0.042 g (35%) of the cyclometallated product [Ru(ttpy)(map)PF₆] (7) and 0.060 g (31%) of the noncyclometallated product [Ru(ttpy)(mapH)(Cl)PF₆] (4). **Non-cyclometallated complex (4):** ¹H NMR (200 MHz, CD₃CN): δ = 8.88 (s, 2 H), 8.54 (d, 2 H, *J* = 7.78 Hz), 8.49 (d, 1 H, *J* = 8.86 Hz), 8.32 (dd, 1 H, *J* = 8.19 Hz), 8.22 (d, 1 H, *J* = 8.23 Hz), 8.08 (d, 2 H, *J* = 8.34 Hz), 7.85 (d, 1 H, *J* = 8.88 Hz), 7.93–7.86 (m, 2 H), 7.77 (d, 1 H, *J* = 1.62 Hz), 7.74 (d, 1 H, *J* = 1.62 Hz), 7.69 (d, 1 H, *J* = 1.65 Hz), 7.52 (d, 2 H, *J* = 8.06 Hz), 7.34–7.25 (m, 3 H), 6.92 (td, 2 H, *J* = 7.24 and 1.34 Hz), 6.36 (dd, 1 H, *J* = 5.92 Hz), 5.34 (d, 1 H, *J* = 2.42 Hz), 3.39 (s, 3 H), 2.50 (s, 3 H). – MS; *m/z* (%): 891 (35) [M – PF₆[–]], 746 (100) [M – 2PF₆[–] + e[–]].

Compound 7: ¹H NMR (200 MHz, CD₂Cl₂): δ = 8.75 (dd, 1 H, *J* = 6.72 Hz, *J* = 1.56 Hz), 8.32 (d, 1 H, *J* = 8.86 Hz), 8.34–8.17 (m, 5 H), 8.10 (s, 2 H), 7.87 (dd, 2 H, *J* = 7.8 Hz, *J* = 1.45 Hz), 7.79 (d, 2 H, *J* = 8.32 Hz), 7.47 (d, 2 H, *J* = 8.06 Hz), 7.37 (dd, 2 H, *J* = 5.38 Hz, *J* = 1.36 Hz), 7.17 (d, 2 H, *J* = 8.34 Hz), 7.11–7.09 (m, 2 H), 6.45 (d, 2 H, *J* = 8.88 Hz), 6.07 (d, 2 H, *J* = 8.60 Hz), 3.52 (s, 3 H), 2.52 (s, 3 H). – MS (FAB-MS) (nitrobenzyl alcohol matrix); *m/z* (%): 855 (40) [M⁺], 710 (100) [M – PF₆[–]].

Ru(dqpy)₂(PF₆)₂ (5): A suspension of Ru(dqpy)Cl₃ (0.070 g, 0.11 mmol) and dqpy (0.049 g, 0.12 mmol) was heated to reflux for 6 h in glacial acetic acid (8 mL) with 2–3 drops of *N*-ethylmorpholine. Yield 0.040 g (30%). – ¹H NMR (200 MHz, CD₂Cl₂): δ = 9.09 (d, 8 H, *J* = 7.88 Hz), 8.24 (d, 8 H, *J* = 10.08 Hz), 8.07 (4 H, *J* = 8.12 Hz), 7.79 (d, 1 H, *J* = 1.48 Hz), 7.75 (t, 2 H, *J* = 1.72 Hz), 7.71 (d, 1 H, *J* = 1.72 Hz), 7.68–7.54 (m, 8 H), 2.56 (s, 6 H). – MS (FAB-MS) (nitrobenzyl alcohol matrix); *m/z* (%): 1093 (15) [M – PF₆[–]], 948 (35) [M – 2PF₆[–] + e[–]].

Ru(dqpy)(mappy)(PF₆)₂ (6): A suspension of Ru(dqpy)Cl₃ (0.08 g, 0.13 mmol) and mappy (0.048 g, 0.13 mmol) was heated to reflux for 5 h in glacial acetic acid (12 mL) with 2–3 drops of *N*-ethylmorpholine. Yield 0.076 g (49%) of **6** as a dark violet solid. – ¹H NMR (300 MHz, CD₂Cl₂): δ = 9.06–8.90 (m, 3 H), 8.70 (s, 2 H), 8.54 (d, 1 H, *J* = 8.76 Hz), 8.39 (d, 2 H, *J* = 8.22 Hz), 8.32 (d, 1 H, *J* = 8.97 Hz), 8.24–8.18 (m, 5 H), 7.83 (td, 3 H, *J* = 1.11 Hz, *J* = 1.26 Hz, *J* = 1.08 Hz), 7.76 (s, 2 H), 7.67–7.52 (m, 7 H), 7.36 (d, 1 H, *J* = 8.22 Hz), 6.60 (d, 2 H, *J* = 8.79 Hz), 6.11 (d, 2 H, *J* = 8.58 Hz), 3.51 (s, 3 H), 2.60 (s, 3 H), 1.96 (s, 3 H). – MS (FAB-MS) (nitrobenzyl alcohol matrix); *m/z* (%): 1047 (80) [M – PF₆[–]], 902 (100) [M – 2PF₆[–] + e[–]], 451 (55) [(M – 2PF₆[–])/2].

Ru(mappy)(dtp)(PF₆)₂ (8): A suspension of Ru(mappy)Cl₃ (0.060 g, 0.10 mmol) and dtpH (0.039 g, 0.10 mmol) was heated to reflux for 3 h in glacial acetic acid (6 mL) with 2–3 drops of *N*-ethylmorpholine. Yield 0.040 g (41%). – ¹H NMR (200 MHz, CD₃CN): δ = 8.57 (d, 1 H, *J* = 2.68 Hz), 8.39–8.27 (m, 4 H), 8.20 (d, 1 H, *J* = 8.86 Hz), 8.09 (d, 1 H, *J* = 8.84 Hz), 7.99 (d, 2 H, *J* = 6.71 Hz), 7.92 (d, 1 H, *J* = 6.2 Hz), 7.82 (d, 2 H, *J* = 7.8 Hz), 7.50 (d, 1 H, *J* = 9.68 Hz), 7.34–7.18 (m, 2 H), 6.59–6.52 (m, 2 H), 6.32 (d, 1 H, *J* = 8.32 Hz), 6.12 (d, 2 H, *J* = 8.31 Hz), 5.87–5.76 (br, 3 H), 5.70 (d, 2 H, *J* = 8.32 Hz), 5.04 (s, 1 H), 3.66 (s, 3 H), 2.08 (s, 3 H), 1.82 (s, 3 H), 1.64 (s, 3 H). – MS (FAB-MS) (nitrobenzyl alcohol matrix); *m/z* (%): 838 (100) [M – PF₆[–]].

Ru(tppy)(dtp)(PF₆)₂ (9): A mixture of Ru(tppy)Cl₃ (0.070 g, 0.13 mmol) and dtpH (0.047 g, 0.13 mmol) was heated to reflux for 3 h in glacial acetic acid (6 mL) with 2–3 drops of *N*-ethylmorpholine. Yield 0.042 g (35%). – ¹H NMR (200 MHz, CD₂Cl₂): δ = 8.39 (s, 2 H), 8.31 (d, 1 H, *J* = 8.32 Hz), 8.24 (d, 2 H, *J* = 7.80 Hz), 8.48–8.20 (m, 4 H), 8.05 (d, 1 H, *J* = 8.86 Hz), 7.96 (d, 2 H, *J* = 8.06 Hz), 7.74 (d, 1 H, *J* = 7.78 Hz), 7.73 (td, 2 H, *J* = 1.48 Hz, *J* = 6.72 Hz), 7.53 (d, 2 H, *J* = 7.8 Hz), 7.30 (d, 2 H, *J* = 8.32 Hz), 7.24 (d, 1 H, *J* = 1.22 Hz), 6.94 (dd, 1 H, *J* = 11.56 Hz, *J* = 1.34 Hz), 6.93 (t, 1 H, *J* = 1.62 Hz), 6.68 (d, 2 H, *J* = 7.8 Hz), 6.57 (dd, 1 H, *J* = 6.72 Hz, *J* = 1.30 Hz), 5.97 (d, 2 H, *J* = 7.8 Hz), 2.53 (s, 3 H), 2.02 (s, 3 H), 1.78 (s, 3 H). – MS (FAB-MS) (nitrobenzyl alcohol matrix); *m/z* (%): 784 (100) [M – PF₆[–]].

Ru(dqpy)(dtp)(PF₆)₂ (10): A suspension of Ru(dqpy)Cl₃ (0.070 g, 0.11 mmol) and dtpH (0.041 g, 0.11 mmol) was heated to reflux for 3 h in glacial acetic acid (10 mL) with 2–3 drops of *N*-ethylmorpholine. Yield: 0.072 g (64%) of **10** as a dark purple solid. – ¹H NMR (300 MHz, CD₂Cl₂): δ = 8.59 (s, 3 H), 8.52 (d, 1 H, *J* = 8.76 Hz), 8.44 (s, 3 H), 8.38 (d, 1 H, *J* = 8.76 Hz), 8.29 (d, 1 H, *J* = 6.96 Hz), 8.26 (d, 1 H, *J* = 6.39 Hz), 8.02 (t, 7 H, *J* = 8.76 Hz, *J* = 7.14 Hz), 7.79 (d, 2 H, *J* = 8.04 Hz), 7.68 (t, 2 H, *J* = 6.93 Hz, *J* = 8.22 Hz), 7.58 (d, 2 H, *J* = 7.86 Hz), 7.50 (td, 2 H, *J* = 1.11 Hz, *J* = 1.11 Hz, *J* = 1.08 Hz), 7.37 (d, 2 H, *J* = 8.4 Hz), 6.75 (d, 2 H, *J* = 7.68 Hz), 6.54 (d, 1 H, *J* = 6.57 Hz), 6.09 (d, 2 H, *J* = 7.86 Hz), 2.61 (s, 3 H), 2.29 (s, 3 H), 2.08 (s, 3 H). – MS (FAB-MS) (nitrobenzyl alcohol matrix); *m/z* (%): 1029 (5) [M⁺], 884(100) [M – PF₆[–]].

X-ray Data Collection: Details concerning the crystal structure are given in Table 4. For all computations the MolEN package was used.^[19] Crystallographic data (excluding structure factors) for the structure reported in this paper have been deposited with the Cambridge Crystallographic Data Centre as supplementary publication no. CCDC-119759. Copies of the data can be obtained free of charge on application to CCDC, 12 Union Road, Cambridge CB21EZ, UK [Fax: (internat.) +44(1223)336-033; E-mail: deposit@ccdc.cam.ac.uk].

Table 4. X-ray experimental data of Ru(tppy)(mapH)(Cl)(PF₆) (4)

Formula	C ₄₁ H ₃₁ N ₅ OCIRu-PF ₆
Molecular mass	891
Color	red
Crystal system	monoclinic
<i>a</i> [Å]	15.378(4)
<i>b</i> [Å]	13.263(3)
<i>c</i> [Å]	20.306(6)
β [deg]	90.54(2)
Volume [Å ³]	4141.4
<i>Z</i>	4
<i>D</i> _{calcd.} [g cm ^{–3}]	1.553
Wavelength [Å]	1.5418
<i>m</i> [cm ^{–1}]	47.206
Space group	<i>P</i> 2 ₁ / <i>c</i>
Diffractionmeter	Philips PW1100/16
Crystal dimensions [mm]	0.30 × 0.20 × 0.10
Temperature [°C]	–100
Radiation (monochromated)	Cu-K _α graphite
Mode	q/2q flying step-scan
Scan speed [deg ^{–1}]	0.020
Step width [deg]	0.05
Scan width [deg]	1.10 + 0.14*tg(<i>q</i>)
Octants	± <i>h</i> + <i>k</i> + <i>l</i>
<i>q</i> _{min/max} [deg]	3/54
Number of data collected	5459
Number of data with <i>I</i> > 3σ(<i>I</i>)	4247
Number of variables	559
Abs _{min/max}	0.89/1.11
<i>R</i> (<i>F</i>)	0.037
<i>R</i> _w (<i>F</i>)	0.062
<i>P</i>	0.08
Largest peak in final diff. [e [–] Å ^{–3}]	0.07
GO _F	1.434

Acknowledgments

This work was performed with financial support from the CNRS (France), CNR (Italy), and the HCM Research Network (Contract no. ERBCH RXCT930145). We thank André De Cian, Nathalie Kyritsakas and Jean Fischer for the X-ray structure and Patrice Staub for his technical assistance.

- [1] [1^a] A. Juris, V. Balzani, F. Barigelletti, S. Campagna, P. Belser, A. Von Zelewsky, *Coord. Chem. Rev.* **1988**, *84*, 85–277. – [1^b] V. Balzani, F. Scandola, *Supramolecular Photochemistry*; Ellis Horwood; Chichester, **1991**. – [1^c] J.-P. Sauvage, J.-P. Collin, J.-C. Chambron, S. Guillerez, C. Coudret, V. Balzani, F. Barigelletti, L. De Cola, L. Flamigni, *Chem. Rev.* **1994**, *94*, 993–1019.
- [2] [2^a] F. Barigelletti, A. Juris, V. Balzani, P. Belser, A. Von Zelewsky, *Inorg. Chem.* **1983**, *22*, 3335–3339. – [2^b] R. S. Lumpkin, E. M. Kober, L. A. Worl, Z. Murtaza, T. J. Meyer, *J. Phys. Chem.* **1990**, *94*, 239–243. – [2^c] P. A. Anderson, G. F. Strousse, J. A. Treadway, F. R. Keene, T. J. Meyer, *Inorg. Chem.* **1994**, *33*, 3863–3864. – [2^d] M. Maestri, N. Armarolio, V. Balzani, E. C. Constable, A. M. W. Cargill Thompson, *Inorg. Chem.* **1995**, *34*, 2759–2767.
- [3] T. J. Meyer, *Pure Appl. Chem.* **1986**, *58*, 1193–1206.
- [4] [4^a] C. R. Hecker, A. K. I. Gushurst, D. R. McMillin, *Inorg. Chem.* **1991**, *30*, 538–541. – [4^b] A. C. Benniston, V. Grosshenny, A. Harriman, R. Ziessel, *Angew. Chem. Int. Ed. Engl.* **1994**, *33*, 1884–1885. – [4^c] G. F. Strousse, J. R. Schoonover, R. Duesing, S. Boyde, W. E. Jones Jr., T. J. Meyer, *Inorg. Chem.* **1995**, *34*, 473–487. – [4^d] N. H. Damauer, T. R. Boussie, M. Devenney, J. K. McCusker, *J. Am. Chem. Soc.* **1997**, *119*, 8253–8268. – [4^e] L. Hammarström, F. Barigelletti, L. Flamigni, M. T. Indelli, N. Armarolio, G. Calogero, M. Guardigli, A. Sour, J.-P. Collin, J.-P. Sauvage, *J. Phys. Chem.* **1997**, *101*, 9061–9069.
- [5] J. A. Treadway, B. Loeb, R. Lopez, P. A. Anderson, F. R. Keene, T. J. Meyer, *Inorg. Chem.* **1996**, *35*, 2242–2246.
- [6] A. P. Zipp, L. A. Sacksteder, J. Streich, A. Cook, J. N. Demas, B. A. DeGraff, *Inorg. Chem.* **1993**, *32*, 5629–5632.

- [7] J.-P. Collin, R. Kayhanian, J.-P. Sauvage, G. Calogero, F. Barigelletti, A. De Cian, J. Fischer, *J. Chem. Soc., Chem. Commun.* **1997**, 775–776.
- [8] [8a] P. Reveco, J. H. Medley, A. R. Garber, N. S. Bhacca, J. Selbin, *Inorg. Chem.* **1985**, *24*, 1096–1099. – [8b] E. C. Constable, J. M. Holmes, *J. Organomet. Chem.* **1986**, *301*, 203–208.
- [9] E. C. Constable, M. J. Hannon, *Inorg. Chim. Acta* **1993**, *211*, 101–110.
- [10] A. Gerli, J. Reedijk, M. T. Lakin, A. L. Spek, *Inorg. Chem.* **1995**, *34*, 1836–1843.
- [11] G. B. Deacon, J. M. Patrick, B. W. Skelton, N. C. Thomas, A. H. White, *Aust. J. Chem.* **1984**, *37*, 929–945.
- [12] M. Beley, S. Chodorowski, J.-P. Collin, J.-P. Sauvage, L. Flamigni, F. Barigelletti, *Inorg. Chem.* **1994**, *33*, 2543–2547.
- [13] J.-P. Collin, M. Beley, J.-P. Sauvage, F. Barigelletti, *Inorg. Chim. Acta* **1991**, *186*, 91–93.
- [14] S. Chardon-Noblat, J.-P. Sauvage, *Tetrahedron* **1991**, *47*, 5123–5132.
- [15] C. O. Dietrich-Buchecker, J. F. Nierengarten, J.-P. Sauvage, N. Armaroli, V. Balzani, L. De Cola, *J. Am. Chem. Soc.* **1993**, *115*, 11237–11244.
- [16] J.-P. Collin, S. Guillerez, J.-P. Sauvage, F. Barigelletti, L. De Cola, L. Flamigni, V. Balzani, *Inorg. Chem.* **1991**, *30*, 4230–4238.
- [17] B. P. Sullivan, D. J. Salmon, T. J. Meyer, *Inorg. Chem.* **1978**, *17*, 3334–3341.
- [18] B. P. Sullivan, J. M. Calvert, T. J. Meyer, *Inorg. Chem.* **1980**, *19*, 1404–1407.
- [19] C. K. Fair In *MolEN, An interactive Intelligent System for Crystal Structure Analysis*, Nonius, Delft, The Netherlands, **1990**.
- [20] [20a] J. N. Demas, G. A. Crosby, *J. Phys. Chem.* **1971**, *75*, 991. – [20b] K. Nakamaru, *Bull. Chem. Soc. Jpn.* **1982**, *55*, 2697.
- [21] F. Barigelletti, L. Flamigni, M. Guardigli, A. Juris, M. Beley, S. Chodorowski-Kimmes, J.-P. Collin, J.-P. Sauvage, *Inorg. Chem.* **1996**, *35*, 136–142.

Received June 11, 1999
[199210]